

# Effect of Brillouin slow light on distributed Brillouin fiber sensors

Lufan Zou, Xiaoyi Bao, Shiquan Yang, Liang Chen, and Fabien Ravet

Fiber Optics Group, Department of Physics, University of Ottawa, 150 Louis Pasteur, Ottawa, Ontario K1N 6N5, Canada

Received May 10, 2006; revised June 22, 2006; accepted June 22, 2006;  
posted July 3, 2006 (Doc. ID 70732); published August 25, 2006

The effect of Brillouin slow light on distributed Brillouin fiber sensors (DBFSs) is studied. We demonstrate Brillouin slow light for a 1.2 ns pulse with peak powers ( $P_S$ ) from 3.3 to 56.2 mW on depletion of the pump power ( $P_P$ ) ranging from 1.3 to 83.2 mW in conventional optical fibers (SMF-28). Experiments show that, when pump power depletion is not negligible, for a given  $P_P$  the Brillouin gain and delay time of a pulse decrease when  $P_S$  increases in a long ( $\geq 10$  km) sensing fiber. The optimum pump beam depletion resulting from strong interaction of the pump and the probe in the fiber provides accurate temperature and strain information at a high spatial resolution. Our study reveals that at low  $P_P$  the spatial resolution error caused by the pulse delay for a DBFS with centimeter spatial resolution is less than 5% of the pulse length. © 2006 Optical Society of America

OCIS codes: 290.5900, 190.5530, 060.5530, 060.2370.

Distributed Brillouin fiber sensors (DBFSs) provide an excellent opportunity for monitoring the structural health of civil engineering structures by allowing measurements to be taken along the fiber rather than at discrete points. One of the main concerns for DBFSs is the effort to improve their spatial resolution by use of short pulses or the combination of cw and pulsed light as a probe beam.<sup>1</sup> Recently, slow light obtained by stimulated Brillouin scattering (SBS) in optical fibers has been of great interest<sup>2,3</sup>; the setup used for the study of slow light was similar to a DBFS based on the Brillouin loss technique,<sup>4</sup> in which two counterpropagating laser beams, a pulsed probe beam and cw pump beam, exchange energy through an induced acoustic field. When the beat frequency of the laser beams matches the acoustic frequency  $\nu_B$ , the probe beam experiences maximum amplification from the pump beam. By measuring the forward pulse signal, one obtains the largest pulse delay; while by measuring the backward signal, namely, the depleted cw pump beam, and scanning the beat frequency of the two lasers, one gets a Brillouin loss spectrum centered about the Brillouin frequency that provides strain, temperature, and spatial information. Recently Thévenaz *et al.*<sup>5</sup> showed that the slow-light effect reduces the available resolution of DBFSs based on their theoretical calculation that assumed that the pump beam experiences a negligible depletion. In fact, for Brillouin slow light a strong cw pump and a weak pulse<sup>2,3</sup> were used to get more pulse time delay, and it is reasonable to neglect the cw pump depletion. However, for a DBFS based on the Brillouin loss technique the cw pump depletion cannot be neglected owing to the strong interaction of the pump and the probe,<sup>1</sup> which is the reason that the local temperature and strain can be measured accurately at high spatial resolution. On the other hand, for Brillouin slow light the pulse durations are generally larger than 15 ns,<sup>1,2</sup> or 2.7 ns with a broadening cw pump spectrum,<sup>6</sup> since the narrow bandwidth of SBS does not allow for narrow pulses to be efficiently delayed.<sup>7</sup> However, the use of nanosec-

ond pulses is a key requirement for realizing centimeter spatial resolution for DBFSs. Thus, DBFSs and Brillouin slow-light performance are opposite in nature: the greater the light delay, the worse the DBFS's accuracy.

In this Letter we demonstrate experimentally that Brillouin slow light for a 1.2 ns pulse with peak powers ( $P_S$ ) from 3.3 to 56.2 mW can be obtained on depletion of pump powers ( $P_P$ ) from 1.3 to 83.2 mW. When the depletion of the pump is not negligible (when the pump and the probe powers are comparable, which is the optimized DBFS regime), the spatial resolution error caused by pulse delay for a DBFS with centimeter spatial resolution is less than 5% of the pulse length.

The configuration for observing slow light via SBS is shown in Fig. 1. Two solid-state lasers operating at 1319 nm were used as light sources. The output of Laser 1 was launched to an electro-optic modulator (EOM) to create a pulse signal. Laser 2 was a cw pump laser. To generate a Stokes pulse that is frequency shifted by precisely  $\nu_B$ , a computer-controlled feedback circuit was applied to the laser drivers. Fiber polarization controllers (FPCs) are inserted at both ends of the sensing fiber to optimize the extinction ratio of the Stokes pulse. The pulses have  $P_S$  from 3.3 to 56.2 mW, while the pump laser has  $P_P$

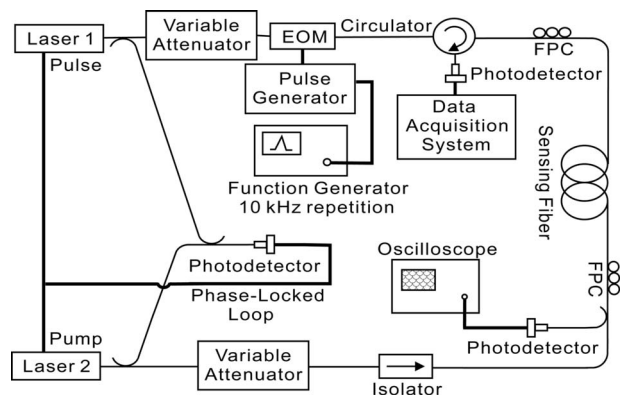


Fig. 1. Experimental setup.

from 1.3 to 83.2 mW before launch into the conventional optical fibers (SMF-28). The 1.2 ns Stokes pulse enters a 10 km long optical fiber, which serves as the slow-light medium and sensing fiber. The output from the isolator counterpropagates through the fiber and serves as the SBS pump beam. The delayed and amplified pulses emerging from the fiber are recorded by using an InGaAs photodiode and a digital oscilloscope. To understand the behavior of the pulse delay in different lengths of the slow-light medium, we also use a 1 km long optical fiber as the slow-light medium in this study. The pulse repetition rate is 10 kHz, which leads single pulse inside the fiber.

Figure 2 shows the temporal evolution of a 1.2 ns Gaussian-shaped pulse in the presence and absence of a 5.1 mW pump beam for the case of input Stokes pulses with a  $P_S$  of 26.3 mW in a 10 km long optical fiber. We used the mass center of the area under the curve for determination of the time delay and Brillouin gain and observed  $\Delta T_d = 0.13$  ns. The pulse delay is clearly observed when the pump beam interacts with the pulse beam. The pulse delay on the falling edge of the pulse is larger than that on the rising edge.

For our sensing application, the pump and the pulse peak powers are around 3.2 and 27.9 mW, respectively.<sup>8</sup> Figure 3 shows the time delay  $\Delta T_d$  as a function of the Brillouin gain for a 1.2 ns pulse duration in 1 and 10 km long optical fibers, where  $P_S$  was fixed at 26.3 mW and the launched  $P_P$  changed from 1.3 mW to 83.2 mW. It is seen that a slow light delay varies linearly with the Brillouin gain and that one can easily control the delay time by changing the pump power  $P_P$ . For 1 and 10 km long sensing fibers the delay rates are 27.3 and 17.1 ps/dB, respectively. In our experiments the measured Brillouin gain includes fiber loss, which is different from the calculated Brillouin gain based on gain parameter  $G = g_B I_p L$ , where  $g_B$  and  $I_p$  are the Brillouin gain coefficient and the pump power intensity in a fiber of length  $L$ .<sup>2,3</sup> For the same launched  $P_P$ , the gain and delay time in the long fiber are larger than those in the short fiber, which implies that the pulse accumu-

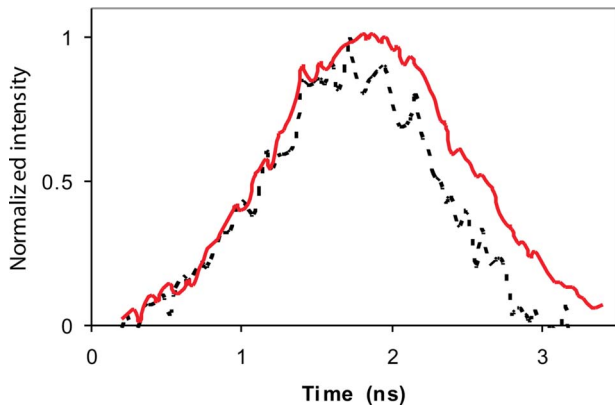


Fig. 2. (Color online) Observation of slow light obtained via SBS in an optical fiber; temporal evolution of the Stokes pulses emitted from the 10 km fiber for  $P_P = 0$  (dotted curve) and  $P_P = 5.1$  mW (solid curve) for 1.2 ns input Stokes pulses with  $P_S = 26.3$  mW.

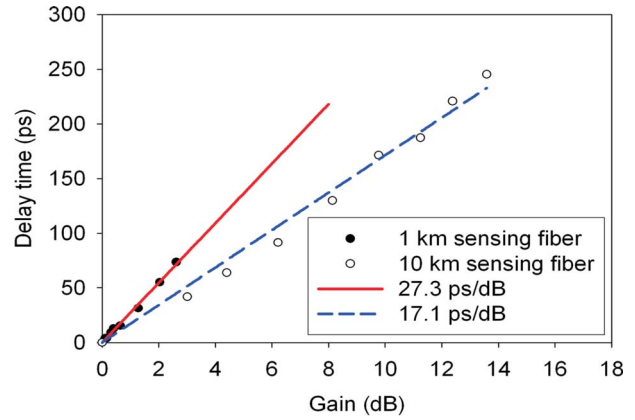


Fig. 3. (Color online)  $\Delta T_d$  as a function of the Brillouin gain for a 1.2 ns pulse in 1 and 10 km sensing fibers ( $P_S = 26.3$  mW, and  $P_P$  was varied from 1.3 mW to 83.2 mW).

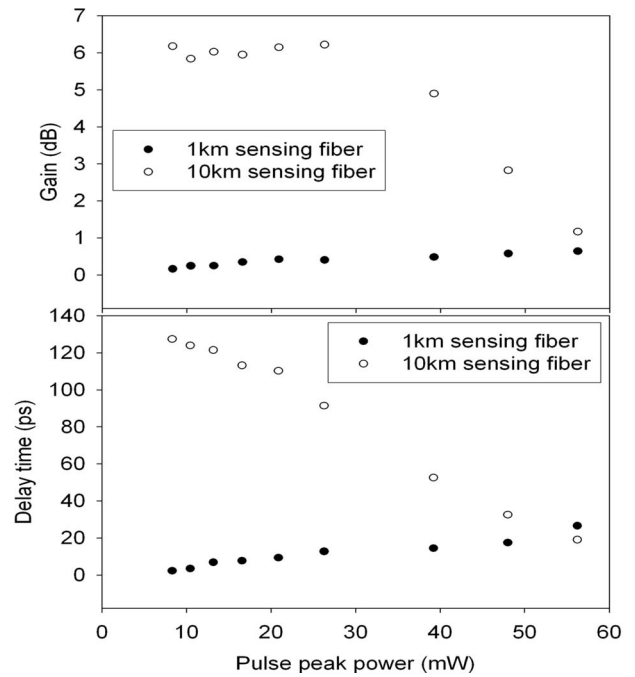


Fig. 4. Delay time and Brillouin gain as a function of  $P_S$  for 1.2 ns pulse in 1 and 10 km sensing fibers, in which  $P_P = 3.2$  mW.

lates energy from the cw that causes the pulse delay to increase during transmission in the fiber. As is shown in Fig. 4, when the launched  $P_P$  was fixed at 3.2 mW, the pulse delay and Brillouin gain as a function of  $P_S$  in a 1 km sensing fiber are much smaller than those in a 10 km sensing fiber. In the 1 km fiber the Brillouin gain increases with  $P_S$ ; thus the pulse delay increases with  $P_S$ . However, in the 10 km fiber the Brillouin gain remains unchanged with  $P_S$  up to a value of 26.3 mW and then drops for higher powers; the delay time decreases with  $P_S$ , which agrees with the numerical study of the pulse delay in optical fiber done by Zhu *et al.*<sup>9</sup> For a strong cw pump and a weak pulsed probe the cw experiences negligible depletion as a result of interaction with the pulse signal.<sup>7</sup> In our experiments the peak powers of the Stokes pulse varied from 3.3 to 56.2 mW, which is higher than or comparable with  $P_P$  of 3.2 mW. Thus the depletion of

the pump power is not negligible. A higher  $P_S$  with a lower gain for the 10 km fiber length in Fig. 4 indicates the existence of the effect of depletion.

To understand the effect of pump depletion as it occurs in a sensing application, we used a 100 m fiber as a sensing medium to measure the backward signal, namely, the cw pump beam. In the 100 m sensing fiber there were ten 2 m sensing sections placed under strain with 1 m of loose fiber separating each sensing section. Figure 5 displays the time domain profile at  $\nu_B=12766$  MHz, in which the peak power of the Stokes pulse was kept at 26.3 mW, while  $P_P$  values were 6.4 mW [curve (a)], 3.2 mW [curve (b)], and 1.6 mW [curve (c)]. For a DBFS based on the Brillouin loss technique, the strong depletion of the pump beam resulting from the strong interaction of the pump and the probe in the fiber provides accurate local temperature and strain information at a high spatial resolution, as shown in Fig. 5(b), which clearly displays ten valleys and nine peaks corresponding to ten strain sections and nine loose sections, respectively. Fine structures in most valleys are attributed to nonuniform strains, which demonstrates that our DBFS achieves centimeter spatial resolution.<sup>1</sup> When  $P_P$  increases to 6.4 mW, the sensing interaction between the pump and the probe becomes weaker compared with the case of 3.2 mW of pump power. Hence the fine structures in most valleys disappear [Fig. 5(a)]. There is an optimum depletion corresponding to a maximum Brillouin gain/loss ratio over the whole fiber length. The depletion represents the contrast in the Stokes signal variation. When  $P_P$  drops to 1.6 mW, that is, when the signal drops, the sensing interaction between the pump and the probe is again weak. Thus the intensity of the depleted signal decreases, and local information can hardly be detected [Fig. 5(c)]. The existence of an optimum pump power can also be seen by comparing the sensing signal at the input and output time locations. The input of  $P_P$  was located at 7500 cm. It is

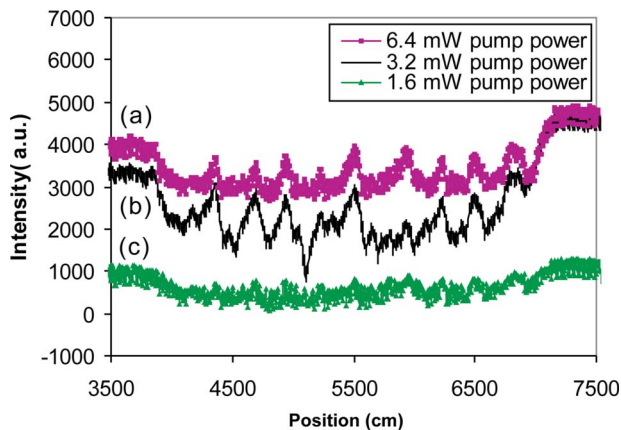


Fig. 5. (Color online) Time domain profile at  $\nu_B=12,766$  MHz, with ten valleys and nine peaks corresponding to ten strain sections and nine loose sections, respectively, in which  $P_S=26.3$  mW and  $P_P$  values were (a) 6.4 mW, (b) 3.2 mW, and (c) 1.6 mW.

clearly shown that the intensity at 7500 cm is higher than that at 3500 cm, which means that the cw pump beam experiences depletion due to interaction of the pulse with the pump. As a result,  $P_P$  drops at 3500 cm. The signal difference between 7500 and 3500 cm is biggest for  $P_P=3.2$  mW but is smaller for  $P_P$  values of 6.4 and 1.6 mW, which means that the depletion contrast of  $P_P$  becomes weaker. Therefore for  $P_S=26.3$  mW and  $P_P=3.2$  mW the strong interaction between the pump and the probe produces moderate pump depletion, which results in accurate detection of strain and temperature by the DBFS. For 3.2 mW of pump power and 26.3 mW of pulse peak power the pulse delay is only 12.7 ps in a 1 km sensing fiber, corresponding to 0.13 cm uncertainty over a 12 cm spatial resolution, which gives an  $\sim 1\%$  uncertainty. For a 10 km long fiber the pulse delay varies from 91.4 to 60.1 ps, giving a maximum 5% uncertainty in location measurement.

In summary, we demonstrate Brillouin slow light experimentally for a 1.2 ns pulse with peak powers from 3.3 to 56.2 mW and pump powers from 1.3 to 83.2 mW. For a given pump power the Brillouin gain and delay time of a pulse decrease when the pulse peak power increases in a long ( $\geq 10$  km) sensing fiber. For the same launched pump power, the gain and delay time of the pulse are proportional to the fiber length. For the Brillouin sensor based on the Brillouin loss technique, the optimum depletion (contrast) of the pump beam resulting from the strong interaction of the pump and the probe in the fibers provides accurate local temperature and strain information at a high spatial resolution, which corresponds to a maximum Brillouin gain/loss ratio over the entire sensing length. Our study reveals that at low pump powers the spatial resolution error caused by the pulse delay for a DBFS with centimeter spatial resolution is less than 5% of the pulse length, which is within the experimental uncertainty.

L. Zou's e-mail address is lzou@uottowa.ca.

## References

1. L. Zou, X. Bao, Y. Wan, and Liang Chen, *Opt. Lett.* **30**, 370 (2005).
2. Y. Okawachi, M. S. Bigelow, J. E. Sharping, Z. Zhu, A. Schweinsberg, D. J. Gauthier, R. W. Boyd, and A. L. Gaeta, *Phys. Rev. Lett.* **94**, 153902 (2005).
3. K. Y. Song, M. G. Herráez, and L. Thévenaz, *Opt. Express* **13**, 82 (2005).
4. X. Bao, D. J. Webb, and D. A. Jackson, *Opt. Lett.* **18**, 1561 (1993).
5. L. Thévenaz, K. Y. Song, and M. G. Herráez, *Opt. Lett.* **31**, 715 (2006).
6. M. G. Herráez, K. Y. Song, and L. Thévenaz, *Opt. Lett.* **14**, 1395 (2006).
7. D. Dahan and G. Eisenstein, *Opt. Express* **13**, 6234 (2005).
8. L. Zou, X. Bao, and Liang Chen, *Opt. Lett.* **28**, 2022 (2003).
9. Z. Zhu, D. J. Gauthier, Y. Okawachi, J. E. Sharping, A. L. Gaeta, R. W. Boyd, and A. E. Willner, *J. Opt. Soc. Am. B* **22**, 2378 (2005).